Microstructural Organization and Macromolecular Contents in Fibrous Tissues of Normal and Hypertensive Eyes with Diffusion Tensor Imaging and Magnetization Transfer Imaging

Leon C. Ho[1,2], Ian A. Sigal[3], Ning-Jiun Jan[3], Tao Jin[1], Ed X. Wu[2], Seong-Gi Kim[1,4], Joel S. Schuman[3], and Kevin C. Chan[1,3]

[1]*Neuroimaging Laboratory, University of Pittsburgh, Pittsburgh, Pennsylvania, United States,* [2]*Department of Electrical and Electronic Engineering, The University of Hong Kong, Pokfulam, Hong Kong, China,* [3]*Departments of Ophthalmology and Bioengineering, University of Pittsburgh, Pittsburgh, Pennsylvania, United States,* [4]*Center for Neuroscience Imaging Research, Institute for Basic Science, Sungkyunkwan University, Suwon, Korea*

Target Audience: Researchers with interests in basic and translational applications of diffusion tensor imaging (DTI) and magnetization transfer imaging (MTI) to study fiber organizations and compositions in healthy and diseased eyes and tendons.

Purpose: The fiber organizations and compositions of the sclera and cornea determine the biomechanical response of the eye to changing intraocular pressures (IOP), and are important in vision-related diseases such as glaucoma [1-3]. However, limited methods have been available to non-invasively and quantitatively determine their exact contributions to the pathogenesis *in vivo* and longitudinally. Recently, our group demonstrated the use of the magic-angle effect to improve MRI sensitivity to reveal T2 and T2* relaxation changes in the scleral and corneal tissues upon IOP loading [4]. In this study, we further evaluated the corneoscleral shells using DTI and MTI at the magic angle in order to test the hypotheses that (1) the microstructural organization and macromolecular contents of the sclera and cornea can be detected and differentiated with high-field MRI; and (2) acute ocular hypertension may alter the DTI and MTI properties in these fibrous tissues.

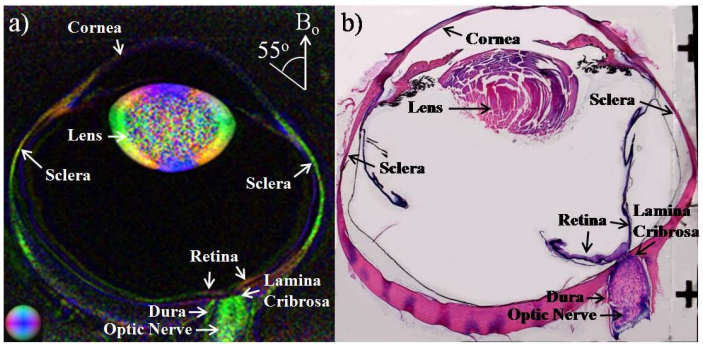

Figure 1. Representative (a) color-coded fractional anisotropy (FA) map (blue: in-out; red: left-right; green: up-down) and (b) hematoxylin and eosin staining of the unloaded whole eye.

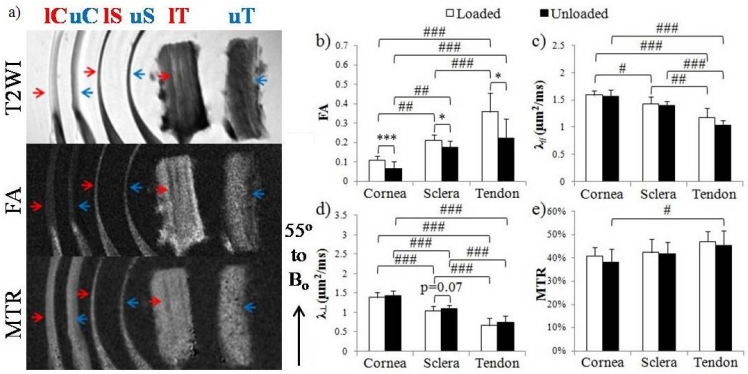

Figure 2. (a) T2-weighted b0 image (T2WI; top), FA map (middle) and magnetization transfer ratio (MTR) map (bottom) of loaded (l; red arrows) and unloaded (u; blue arrows) cornea (C), sclera (S) and tendon (T) tissue section pairs orientated about the magic angle at ~55° to B_o. Quantitative comparisons of (b) FA, (c) axial diffusivity ($\lambda_{//}$), (d) radial diffusivity ($\lambda_{\perp}$) and (e) magnetization transfer ratio (MTR) between loaded and unloaded cornea, sclera and tendon sections at magic angle. (Two-tailed paired t-tests between loaded and unloaded tissues: *p<0.05, ***p<0.001; one-way ANOVA and post-hoc Tukey's tests: #p<0.05, ##p<0.01, ###p<0.001).

Methods: ***Tissue preparation:*** Eight pairs of ovine eyes were extracted and fixed within 24 hours of death. One eye of each ovine was loaded at IOP =50 mmHg using a gravity perfusion system to mimic ocular hypertension and the contralateral eye remained unloaded [4]. Seven pairs of eyes were then washed in PBS and dissected for scleral and corneal tissue sections. The remaining 2 eyes were kept intact for whole eye MRI and hematoxylin and eosin staining. Thirteen ovine Achilles tendons (4 stretch-loaded and 9 unloaded) [4] from the same set of animals were dissected to isolate thin strips and act as positive controls given the shared structural compositions between the tendon and corneoscleral shell. ***MRI protocol:*** Contralateral eyes and tendons from the same sheep were paired up and oriented near the magic angle at ~55° relative to the static magic field (B_o) in a 9.4-Tesla/31-cm Varian/Agilent scanner. DTI and MTI were performed to the whole eye as well as the eye and tendon tissue sections using a 32mm transmit-receive volume coil with fast spin-echo sequences. Imaging parameters included: (i) DTI: two non-diffusion-weighted (b0) images and diffusion weighting at 12 gradient directions at b=500s/mm^2 for whole eye and b=1000s/mm^2 for sectioned tissues; δ/Δ=5/12ms (whole eye) and 5/17ms (tissue sections); TR/TE=2300/21.6ms (whole eye) and 2300/27.8ms (tissue sections); ETL=8; NEX=4; (ii) MTI: 9.5μT saturation pulses at 6000Hz off-resonance; TR/TE=1500/8.43ms; ETL=8; and NEX=5. Both DTI and MTI shared the same slice geometry, with in-plane resolution=140×140μm^2 (whole eye) and 125×125μm^2 (tissue sections), and slice thickness=1mm. ***Data Analysis:*** DTI paramatric maps including fractional anisotropy (FA), axial diffusivity ($\lambda_{//}$), radial diffusivity ($\lambda_{\perp}$) and mean diffusivity (MD) maps were computed using DTIStudio. Magnetization transfer ratio (MTR) was calculated by the equation, $(M_0-M_{sat})/M_0$ where M_{sat} and M_0 are signals with and without saturation pulse respectively. Regions of interest were manually drawn and measured on the cornea, sclera and tendon near the magic angle (Fig. 2a arrows).

Results: In the color-encoded FA map (Fig. 1a), the principal orientations of various tissues in the eye including the sclera, cornea, lens, retina, optic nerve and dura generally matched with fiber arrangements in hematoxylin and eosin staining (Fig. 1b). In the tissue sections (Fig. 2a), different T2-weighted signals and FA and MTR profiles were observed near the magic angle among loaded and unloaded sclera, cornea and tendons. Consistent with our previous study [4], T2-weighed (b_0) signals were higher in loaded than unloaded tissues at magic angle (one-tailed paired t-tests, p<0.05; not shown). DTI quantitation in Figs. 2b-d showed the highest FA and lowest directional diffusivities ($\lambda_{//}$ and $\lambda_{\perp}$) in tendon followed by sclera and cornea. Loaded tissues also showed significantly higher FA than unloaded tissues. A trend of lower $\lambda_{\perp}$ was observed in loaded sclera than unloaded sclera (p=0.07). In Fig. 2d, the tendon appeared to show the highest MTR followed by sclera and cornea, with MTR in unloaded tendon being significantly higher than unloaded cornea. However, no significant difference in MTR were found between loaded and unloaded tissues.

Discussion: In DTI of unloaded tissues, the principal orientations of the corneoscleral shell revealed in the color-encoded FA map (Fig. 1a) generally matched with histological staining and with the fiber arrangements reported in the literature [5]. The highest FA observed in tendon was consistent with the parallel alignment of tendon collagen fibrils to the long axis [6]. Although fibers in the corneoscleral shell are highly aligned, they may traverse each other in slightly different directions to provide maximal mechanical strength within the curved globe [5,7]. Such crossing fibers may lead to lower FA in ocular tissues compared to the tendon. The highest directional diffusivities ($\lambda_{//}$ and $\lambda_{\perp}$) in cornea may likely reflect the rich water content and more regular lattice arrangement in the corneal stroma followed by sclera and tendon [8]. Upon pressure loading, the collagen-rich tissues experienced stretch and compression leading to fiber straightening [1] and a more anisotropic microstructural environment. Our results suggested that FA is a more sensitive DTI marker than $\lambda_{//}$ and $\lambda_{\perp}$ to pressure loading in ocular tissues and tendons. MTR in unloaded tendon was slightly higher than unloaded sclera and significantly higher than unloaded cornea. This may be explained by the most abundant collagen contents in tendon (~100% dry mass) compared to sclera and cornea (~70-80% dry weight) [9]. The insignificant MTR difference between loaded and unloaded tissues may suggest no apparent alteration in macromolecular contents despite microstructural changes upon acute pressure loading [2].

Conclusions: Our DTI and MTI results demonstrated the significant differences in microstructural organization and macromolecular contents among unloaded cornea, sclera and tendon tissues. In addition, acute pressure loading altered the microstructures in ocular tissues and tendons with no apparent changes in macromolecular contents. DTI and MTI may open up new avenues for cross-sectional and longitudinal monitoring of the biomechanical and biochemical properties of ocular fiber organization and remodeling in aging and diseases involving the corneoscleral shell such as acute and chronic ocular hypertension, glaucoma and myopia.

References: [1] Sigal I.A., IOVS, 2014; [2] Pijanka J.K., IOVS, 2014; [3] Quigley H., ARVO:1665, 2014 [4] Ho L.C., IOVS 2014; [5] Pijanka J.K., IOVS, 2012; [6] Fulleron G.D., JMRI, 2007; [7] Meek K.M., Exp Eye Res, 2004; [8] Dohlman C.H., Acta Ophthalmol, 1955; [9] Maurice DM. The Cornea and Sclera. 3rd ed. New York: Academic Press; 1984;